COBEM 2023 27TH INTERNATIONAL CONGRESS OF MECHANICAL ENGENEERING

ABCM Brazilian Society of Mechanical Sciences and Engineering
27th ABCM International Congress of Mechanical Engineering
December 04-08, 2023, Florianópolis-SC, Brazil

COB-2023-0902
Onset of growth of Saffman-Taylor instabilities in a three-layer, rectangular Hele-Shaw flow

Pedro H. A. Anjos
Carlos R. Hollanda
Rafael M. Oliveira
Departamento de Engenharia Mecânica, Pontifícia Universidade Católica do Rio de Janeiro, Rio de Janeiro RJ 22451-900, Brazil
pamorimanjos@esp.puc-rio.br, carlos.hollanda@yahoo.com.br, rmo@puc-rio.br

Abstract. *We investigate the formation of Saffman-Taylor instabilities in a three-layer, rectangular Hele-Shaw flow, where an intermediate body of fluid is bounded by two interfaces and separates the left and rightmost fluid regions. In this system, the two interfaces interact with one another, and the intermediate fluid thickness regulates the coupling strength between them. We approach the problem perturbatively through linear stability analysis and derive a set of coupled, first-order ordinary differential equations for the disturbances emerging on the interfaces. Then, this set of equations is solved analytically and utilized to investigate the influence of the intermediate fluid thickness on the Saffman-Taylor instabilities at the onset of their formation, i.e., at the early time regime of the flow. The results obtained in our work provide important insights applicable to enhanced oil recovery (EOR) strategies, in particular, to chemical methods in which two (treatment and post-treatment) fluids are pumped in sequence into the porous rock during oil recovery processes.*

Keywords: *Hele-Shaw cell, viscous fingering, three-phase flow, linear stability analysis*

1. INTRODUCTION

The development of Saffman-Taylor instabilities (Saffman and Taylor (1958)) in Hele-Shaw cells is a classical fluid mechanics problem that became a prototypical example of moving interface, pattern-forming phenomena. A rectangular Hele-Shaw cell is an experimental device consisting of two parallel glass plates separated by a narrow gap which, in its traditional setup (Bensimon *et al.* (1986); Homsy (1987); Howison (1992); McCloud and Maher (1995)), is filled with a single viscous fluid. When a less-viscous fluid is injected into the more viscous one in this geometry, the initially flat fluid-fluid interface separating the two fluids destabilizes. The interface deforms, and different Fourier modes grow and compete dynamically, leading to undulated, finger-like patterned structures. These viscous fingering patterns arise due to the Saffman-Taylor instability, which is triggered by the viscosity difference between the fluids.

The two-fluid, single-interface Hele-Shaw setting has been actively investigated over the past decades motivated by scientific and practical interests. Nevertheless, a much less explored variation of this traditional Saffman-Taylor problem concerns the simultaneous flow of three fluids. In contrast to its simpler two-fluid counterpart, three-fluid flows involve the presence of two interacting interfaces, adding complexity and new behaviors to the hydrodynamical system. In addition, multiple-interface Hele-Shaw configurations have been gaining more attention recently because of their connection with a particular method employed in the oil industry known as chemical-enhanced oil recovery. While studies of three-fluid Hele-Shaw flows are less prevalent in the literature than the two-fluid problem, a few analytical, numerical and experimental studies of such a multiple-interface configuration have been undertaken. For example, linear (Gin and Daripa (2015, 2021a,b)) and weakly nonlinear analyses (Anjos and Li (2020)) have been employed to study the radial displacement of three fluids in a Hele-Shaw cell. Numerical simulation employing boundary integrals (Zhao *et al.* (2020)) and level set (Morrow *et al.* (2023)) methods have also been utilized for this type of geometry, and the studies conducted by Cardoso and Woods (1995) and Ward and White (2011) focused on experimental investigations.

Other variations of the three-fluid, radial flow mentioned above have also been reported in the literature, such as the experiments in rotating Hele-Shaw cells (Carrillo *et al.* (1999, 2000)) and, more recently, the three-fluid flows with magnetic liquids (Livera *et al.* (2021, 2022); Coutinho and Miranda (2022)) driven by applied magnetic field configurations. However, our interest in this paper is to theoretically investigate the emergence of Saffman-Taylor instabilities during three-fluid flow in a rectangular Hele-Shaw cell geometry, a topic that the scientific community has relatively neglected. A noteworthy exception is the study conducted by Jackson (2021), who investigated the problem utilizing level set numerical simulations. Although a linear stability analysis was also provided, the work performed by Jackson (2021) focused on the advanced-time, fully nonlinear regime of the dynamics. Therefore, here we intend to revisit the problem with a focus on the early-time regime. In particular, we will consider the circumstance in which there is an initially unstable interface coupled to an initially stable interface. By utilizing linear stability analysis, we aim to unveil the impact of the stable interface on the early-time dynamics of the unstable one as the coupling strength increases.

The remainder of this paper is structured as follows. In Sec. 2, we derive a set of coupled differential equations that

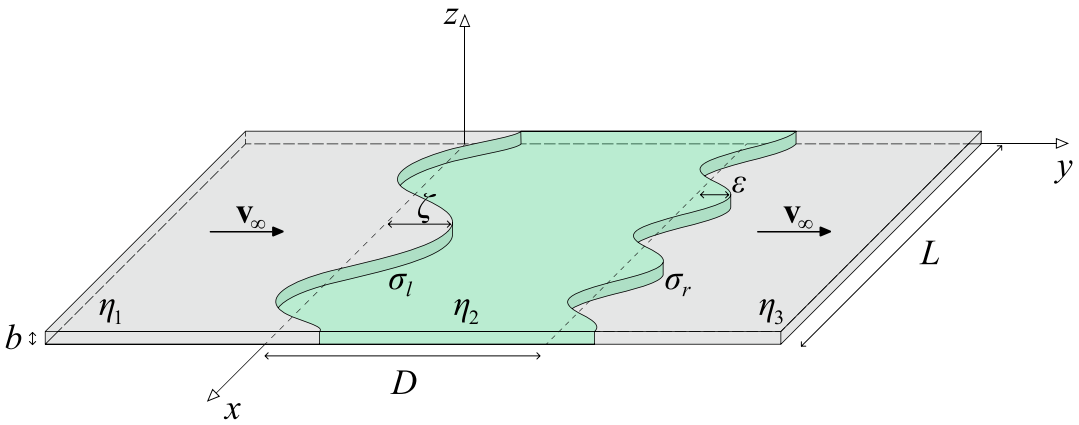

Figure 1. Schematic configuration of the three-fluid flow problem in a horizontal, rectangular Hele-Shaw cell of gap thickness b. The constant external flow velocity is given by $\mathbf{v}_\infty$ and the viscosities of the three fluids involved are denoted as η_1, η_2, and η_3, with $\eta_1 = \eta_3 \ll \eta_2$. Between fluids 1 and 2 lies the initially flat left interface located at $y = 0$ (represented by a dashed line), with its perturbed shape described by $y_l = \zeta(x,t)$, where $0 \leq x \leq L$. Likewise, between fluids 2 and 3 lies the initially flat right interface located at $y = D$ (represented by a dashed line), with its perturbed shape described by $y_r = D + \varepsilon(x,t)$. The surface tensions of the left and rightmost interfaces are represented as $\sigma_l = \sigma_r = \sigma$.

describes the time evolution of the interfacial perturbation amplitudes for both the left and right interfaces under injection-driven rectangular Hele-Shaw flow displacements. In Sec. 3, we define the growth rates of our problem and utilize them to explore the early-time dynamics and the impact of one interface on the other. Finally, in Sec. 4, we summarize our main results and provide concluding remarks.

2. GOVERNING EQUATIONS AND LINEAR DYNAMICS OF INTERFACIAL PERTURBATIONS

The physical system of interest, depicted in Fig. 1, consists of a horizontal, rectangular Hele-Shaw cell of gap thickness b containing three immiscible, Newtonian, viscous fluids. The viscosities of the left and rightmost fluids are denoted as η_1 and η_3, respectively. In addition, these semi-infinite fluid regions are separated by a finite, intermediate fluid domain of viscosity η_2. In this setting, fluid 1 is injected at constant external flow velocity $\mathbf{v}_\infty = v_\infty \hat{\mathbf{y}}$ at $y = -\infty$, and displaces fluids 2 and 3. Note that the latter is withdrawn at the same velocity at $y = +\infty$. Between fluids 1 and 2 (2 and 3) there is an interface with surface tension σ_l (σ_r). We describe the system in a frame moving with velocity $\mathbf{v}_\infty$ so that the two interfaces may deform, but the leftmost one does not displace from $y = 0$ on average. Likewise, the rightmost interface does not displace from $y = D$ on average. During the flow, the perturbed shapes of the left and right interfaces are described, respectively, by $y_l = \zeta(x,t)$ and $y_r = D + \varepsilon(x,t)$, where

$$\zeta(x,t) = \sum_{k \neq 0} \zeta_k(t)\, e^{ikx} \qquad \text{and} \qquad \varepsilon(x,t) = \sum_{k \neq 0} \varepsilon_k(t)\, e^{ikx} \tag{1}$$

are net perturbations in the form of Fourier expansions, while $\zeta_k(t) = \frac{1}{L}\int \zeta(x,t) e^{-ikx} dx$ and $\varepsilon_k(t) = \frac{1}{L}\int \varepsilon(x,t) e^{-ikx} dx$ are complex Fourier mode amplitudes with wave numbers k, and $0 \leq x \leq L$. The expansions (1) include all possible modes k, with the exception of $k = 0$ since we are in a co-moving frame. The wave vectors are constrained to lie on the x-axis but can be either positive or negative. We apply periodic boundary conditions in x limiting the wave number k to discrete allowed values $2\pi n/L$, for integer n.

In this quasi-two-dimensional setting, our hydrodynamic problem is described by Darcy's law (Saffman and Taylor (1958); Bensimon *et al.* (1986); Homsy (1987); Howison (1992); McCloud and Maher (1995))

$$\mathbf{v}_j + \mathbf{v}_\infty = -\frac{b^2}{12\eta_j} \boldsymbol{\nabla} p_j, \tag{2}$$

and the gap-averaged incompressibility condition

$$\boldsymbol{\nabla} \cdot \mathbf{v}_j = 0, \tag{3}$$

where $\mathbf{v}_j$ and p_j represent, respectively, the gap-averaged velocity and pressure in fluid j (with $j = 1, 2,$ or 3). The interfacial motions are determined by the governing equations (2) and (3), supplemented with two boundary conditions at each fluid-fluid interface. For the leftmost interface between fluid layers 1 and 2, the first set of conditions is given by the pressure jump, Young-Laplace, boundary condition due to surface tension σ_l, and by the kinematic boundary

condition (Saffman and Taylor (1958); Bensimon *et al.* (1986); Homsy (1987); Howison (1992); McCloud and Maher (1995)) which states that the normal components of each fluid's velocity are continuous across the left interface. These are respectively given by

$$(p_1 - p_2)|_{y=y_l} = \sigma_l \kappa|_{y=y_l} \qquad \text{and} \qquad (\mathbf{v}_1 \cdot \hat{\mathbf{n}})|_{y=y_l} = (\mathbf{v}_2 \cdot \hat{\mathbf{n}})|_{y=y_l}. \tag{4}$$

Similarly, the second set of boundary conditions acting on the rightmost interface is

$$(p_2 - p_3)|_{y=y_r} = \sigma_r \kappa|_{y=y_r} \qquad \text{and} \qquad (\mathbf{v}_2 \cdot \hat{\mathbf{n}})|_{y=y_r} = (\mathbf{v}_3 \cdot \hat{\mathbf{n}})|_{y=y_r}. \tag{5}$$

In Eqs. (4) and (5),

$$\kappa = \left(\frac{\partial^2 y}{\partial x^2}\right)\left[1 + \left(\frac{\partial y}{\partial x}\right)^2\right]^{-3/2} \tag{6}$$

is the interfacial curvature in the x-y plane, while $\hat{\mathbf{n}}$ is the unit normal vector at the interfaces.

In order to perform a linear stability analysis of our problem, we first note that the irrotational nature observed in the bulk of each fluid, $\boldsymbol{\nabla} \times \mathbf{v}_j = 0$, allows definition of velocity potentials, $\mathbf{v}_j = -\nabla\phi_j$. Therefore, because the flow is incompressible, we can restate the problem in terms of Laplacians, $\nabla^2\phi_j = 0$. Then, we perform Fourier expansions for these velocity potentials and use the kinematic boundary conditions to express the Fourier coefficients in terms of the perturbations ζ_k and ε_k. Lastly, we substitute the resulting relations and the pressure jump conditions into Darcy's law [Eq. (2)]. Keeping only the first-order terms in ζ and ε, we obtain, after Fourier transforming, the set of coupled equations of motion for both the perturbation amplitudes ζ_k and ε_k

$$\dot{\zeta}_k = f_1(k)\Lambda(k)\zeta_k + f_2(k)\Gamma(k)\varepsilon_k, \tag{7}$$

$$\dot{\varepsilon}_k = f_3(k)\Lambda(k)\zeta_k + f_4(k)\Gamma(k)\varepsilon_k, \tag{8}$$

where

$$\Lambda(k) = \left[v_\infty - \frac{\sigma b^2 k^2}{12\eta_2}\right]|k|, \tag{9}$$

$$\Gamma(k) = \left[v_\infty + \frac{\sigma b^2 k^2}{12\eta_2}\right]|k|, \tag{10}$$

$$f_1(k) = -f_4(k) = \coth(|k|D), \tag{11}$$

and

$$f_2(k) = -f_3(k) = -\frac{1}{\sinh(|k|D)}. \tag{12}$$

We stress that Eqs. (7) and (8) are in agreement with previous expressions obtained by Jackson (2021) for the stability of a viscous blob moving through a Hele-Shaw channel. Additionally, it should be pointed out that in order to obtain Eqs. (7)-(12), we have considered the physical situation in which fluids 1 and 3 are equal and have negligible viscosity, i.e., $\eta_1 = \eta_3 \ll \eta_2$. Under this assumption, the left interface has a positive viscosity contrast, $A_{12} \equiv (\eta_2 - \eta_1)/(\eta_2 + \eta_1) \approx 1$, while the right interface has a negative viscosity contrast, $A_{23} \equiv (\eta_3 - \eta_2)/(\eta_3 + \eta_2) \approx -1$. Nevertheless, we call the readers' attention to the fact that, in opposition to the two-fluid displacement problem, in the three-fluid flow system one cannot conclude that an interface is stable because of its negative viscosity contrast. The two interfaces are coupled, with the coupling strength increasing for lower values of D. Thus, the unstable boundary associated with $A_{12} = 1$ can induce the emergence of instabilities on the interface associated with a negative viscosity jump. The opposite is also true, i.e., a stable interface can also impact the dynamics of an unstable boundary. Eqs. (7) and (8) form a system of coupled first-order ODEs with constant (in time) coefficients that can be solved easily by first isolating ε_k in Eq. (7) and then substituting it in Eq. (8).

In the next section, we will define linear dispersion relations for the two interfaces of our problem in terms of the expressions (7)-(12) found above. That will be the starting point of our linear stability analysis of this three-fluid flow. As it will become clearer in the course of this paper, such an analysis will allow us to extract key insights about the influence of the right interface on the linear dynamics of the left boundary.

3. DISCUSSION

At the linear regime of the dynamics, key insights related to our hydrodynamical problem can be extracted directly from the analysis of the growth rates associated with each interfacial perturbation ζ and ε. For our system, the growth rates are defined as follows

$$\lambda_l(k,t) \equiv \frac{\dot{\zeta}_k}{\zeta_k} = f_1(k)\,\Lambda(k) + f_2(k)\,\Gamma(k)\frac{\varepsilon_k(t)}{\zeta_k(t)}, \tag{13}$$

and

$$\lambda_r(k,t) \equiv \frac{\dot{\varepsilon}_k}{\varepsilon_k} = f_3(k)\,\Lambda(k)\frac{\zeta_k(t)}{\varepsilon_k(t)} + f_4(k)\,\Gamma(k). \tag{14}$$

Here, our goal is to analyze the impact of the initially stable rightmost interface on the early-time dynamics of the initially unstable leftmost interface as the coupling strength between them increases, or equivalently, as the distance D decreases. However, before delving into this specific three-fluid flow problem, we first analyze the situation in which the two interfaces do not interact. Such a situation occurs when the interfaces are very far apart and have been referred to in the literature as the *two-fluid, single-interface limit* (Anjos and Li (2020); Zhao *et al.* (2020); Livera *et al.* (2021, 2022)). This scenario corresponds to setting $D \to \infty$ in Eqs. (13) and (14). This results in the following simplified growth rates

$$\lambda_l(k) = f_1(k)\,\Lambda(k) = \left[v_\infty - \frac{\sigma b^2 k^2}{12\eta_2}\right]|k|, \tag{15}$$

and

$$\lambda_r(k) = f_4(k)\,\Gamma(n) = -\left[v_\infty + \frac{\sigma b^2 k^2}{12\eta_2}\right]|k|. \tag{16}$$

Note that under this circumstance, we obtain time-independent growth rates, in contrast to the time-dependent ones, Eqs. (13) and (14), obtained for coupled interface with finite D. Furthermore, by inspecting Eq. (15) it becomes evident that the growth rate of the left interface results from the balance between the destabilizing effect related to the velocity v_∞ and the stabilizing contribution coming from surface tension σ. Therefore, the left interface is unstable [$\lambda_l(k) > 0$] for wave numbers, k, within the interval $0 \leq k \leq k_c$, where $k_c = \sqrt{12\eta_2 v_\infty/\sigma b^2}$ is the critical wave number, found by setting $\lambda_l(k) = 0$. On the other hand, one can observe that the right interface is always stable [$\lambda_r(k) < 0$] no matter the value of k. This is because the viscosity jump associated with the right interface is negative ($A_{23} = -1$), turning the flow stable against small amplitude perturbations. Because the interfaces are decoupled ($D \to \infty$), this stable flow does not change over time. We stress that these *two-fluid, single-interface limit* conclusions, as well as expressions (15) and (16), are in agreement with previously reported linear stability results obtained by previous works on two-fluid, rectangular Hele-Shaw displacement flows (Miranda and Widom (1998)).

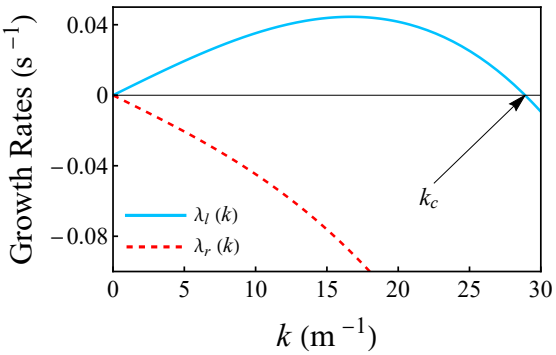

Figure 2. Linear growth rates $\lambda_l(k)$ [see Eq. (15)] and $\lambda_r(k)$ [see Eq. (16)] as a function of wave number k for $D \to \infty$. In addition, we set $b = 3 \times 10^{-3}$ m, $v_\infty = 4 \times 10^{-3}$ m/s, $\eta_2 = 7.36 \times 10^{-3}$ Pa s, and $\sigma = 47 \times 10^{-3}$ N/m. The black straight arrow points to the critical wave number k_c that defines the band of unstable modes for the left interface.

In order to better illustrate the conclusions obtained from the direct analysis of Eqs. (15) and (16), and also to present the typical growth rate curve obtained from a linear stability analysis, in Fig. 2, we plot the growth rates $\lambda_l(k)$ [Eq. (15)] and $\lambda_r(k)$ [Eq. (16)] as a function of the wave number k for $D \to \infty$. This is done considering the physical parameters $b = 3 \times 10^{-3}$ m, $v_\infty = 4 \times 10^{-3}$ m/s, $\eta_2 = 7.36 \times 10^{-3}$ Pa s, and $\sigma = 47 \times 10^{-3}$ N/m. Fig. 2 confirms the predictions obtained from Eqs. (15) and (16) discussed in the previous paragraph. Furthermore, we indicate with a black straight arrow the critical wave number k_c, which defines the band of unstable modes for the left interface. Note that such a

wave number plays an important role at the linear level of the dynamics, as it delimits the possible wavelengths that may manifest on the left interface during three-fluid flow experiments. Therefore, to access the right interface's effects on the left interface's early-time dynamics, we will focus our analysis on the variation of k_c as the initial distance D between the interfaces decreases.

In Fig. 3, we show variations of the left interface's critical wave number k_c as a function of time t for different values of D. Cases associated with finite values of D are represented by dots and are obtained by utilizing the linear dispersion relations (13) and (14). For reference, we display by a black line the time-independent k_c of the $D \to \infty$ case, which was discussed in Fig. 2. All the remaining physical parameters are identical to those utilized in Fig. 2. First, one can observe that finite values of D are always associated with a time-dependent, critical wavenumber, k_c. Furthermore, lower values of D considerably diminish the magnitude of k_c, thus decreasing the band of unstable modes. Such observations suggest that, at the linear level, the right interface impacts the left one by decreasing the number of viscous fingers formed. This stabilizing effect is particularly strong at initial times but diminishes as time progress, with all the cases approaching the value of k_c observed in the decoupled, single-interface situation (for $D \to \infty$). Fig. 3 also reveals that, for $D = 6$ cm, one observes a short period in which k_c is zero, indicating a complete absence of instabilities on the left interface, even with a very large positive viscosity contrast (≈ 1). Nevertheless, this effect only delays but does not entirely prevent the growth of viscous fingering.

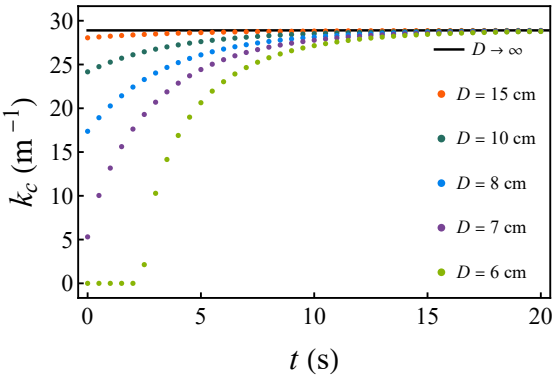

Figure 3. Left interface's critical wave number k_c as a function of time t for $D = 6$ cm, $D = 7$ cm, $D = 8$ cm, $D = 10$ cm, $D = 15$ cm, and $D \to \infty$. Cases associated with finite values of D are represented by dots, while the situation for $D \to \infty$ is illustrated by a solid line. All the other physical parameters are identical to those utilized in Fig. 2. A closer proximity (smaller D values) between the interfaces narrows the band of unstable modes for the unstable left interface.

4. CONCLUSION

We have investigated the problem of the immiscible displacement of an intermediate, finite viscous fluid layer, bounded on the left and the right by semi-infinite fluids of negligible viscosity flowing in the confined geometry of a horizontal, rectangular Hele-Shaw cell. This particular hydrodynamic setup is of special interest because (i) it involves the interplay between two coupled interfaces (here, denoted as the left and right boundaries) of a doubly connected fluid region and (ii) it is related to chemically enhanced oil recovery strategies where at least three fluids are pumped in sequence into oil wells for oil recovery.

In this work, our primary goal was to analyze the impact of the initially stable, right interface (viscosity contrast ≈ -1) on the early-time dynamics of the initially unstable, left interface (viscosity contrast ≈ 1) as the coupling strength increases. Utilizing a Darcy-law-based flow description, we tackled the problem theoretically by employing a perturbative linear stability analysis of this dual-interface system. A set of coupled differential equations of motion for the interfacial instabilities emerging on each boundary was derived and, together with its analytical solutions, were utilized to define the linear growth rates of the system.

Our linear stability results have shown that the two interfaces are coupled already at the linear regime. Furthermore, we have found that the interaction of these two fronts is regulated by the distance D between the initially unperturbed interfaces. Additionally, we have verified that, for lower values of D, the initially stable interface impacts the unstable one by decreasing the number of viscous fingers formed. Such a stabilizing effect was found to be more intense at initial times of the flow but diminishes as time advances. Furthermore, if D is sufficiently small, we have found that viscous fingering formation is completely suppressed for a short period of time, even for very large viscosity contrast.

5. ACKNOWLEDGEMENTS

P. H. A. Anjos and R. M. Oliveira acknowledge support of the Brazilian National Agency for Petroleum, Natural Gas and Biofuels through the Human Resources Program, PRH-ANP, under Grant No. 01.19.0248.00, Ref. No. 0420/19. C. R. Hollanda wishes to thank CAPES for financial support.

6. REFERENCES

Anjos, P.H. and Li, S., 2020. "Weakly nonlinear analysis of the saffman-taylor problem in a radially spreading fluid annulus". *Physical Review Fluids*, Vol. 5, No. 5, p. 054002.

Bensimon, D., Kadanoff, L.P., Liang, S., Shraiman, B.I. and Tang, C., 1986. "Viscous flows in two dimensions". *Reviews of Modern Physics*, Vol. 58, No. 4, p. 977.

Cardoso, S.S.S. and Woods, A.W., 1995. "The formation of drops through viscous instability". *Journal of Fluid Mechanics*, Vol. 289, p. 351–378. doi:10.1017/S0022112095001364.

Carrillo, L., Soriano, J. and Ortın, J., 1999. "Radial displacement of a fluid annulus in a rotating Hele–Shaw cell". *Physics of Fluids*, Vol. 11, No. 4, pp. 778–785. ISSN 1070-6631. doi:10.1063/1.869950. URL https://doi.org/10.1063/1.869950.

Carrillo, L., Soriano, J. and Ortın, J., 2000. "Interfacial instabilities of a fluid annulus in a rotating Hele–Shaw cell". *Physics of Fluids*, Vol. 12, No. 7, pp. 1685–1698. ISSN 1070-6631. doi:10.1063/1.870419. URL https://doi.org/10.1063/1.870419.

Coutinho, I.M. and Miranda, J.A., 2022. "Field-controlled flow and shape of a magnetorheological fluid annulus". *Phys. Rev. E*, Vol. 106, p. 025105. doi:10.1103/PhysRevE.106.025105. URL https://link.aps.org/doi/10.1103/PhysRevE.106.025105.

Gin, C. and Daripa, P., 2015. "Stability results for multi-layer radial Hele-Shaw and porous media flows". *Physics of Fluids*, Vol. 27, No. 1. ISSN 1070-6631. doi:10.1063/1.4904983. URL https://doi.org/10.1063/1.4904983. 012101.

Gin, C. and Daripa, P., 2021a. "Stability results on radial porous media and Hele-Shaw flows with variable viscosity between two moving interfaces". *IMA Journal of Applied Mathematics*, Vol. 86, No. 2, pp. 294–319. ISSN 0272-4960. doi:10.1093/imamat/hxab001. URL https://doi.org/10.1093/imamat/hxab001.

Gin, C. and Daripa, P., 2021b. "Time-dependent injection strategies for multilayer hele-shaw and porous media flows". *Phys. Rev. Fluids*, Vol. 6, p. 033901. doi:10.1103/PhysRevFluids.6.033901. URL https://link.aps.org/doi/10.1103/PhysRevFluids.6.033901.

Homsy, G.M., 1987. "Viscous fingering in porous media". *Annual review of fluid mechanics*, Vol. 19, No. 1, pp. 271–311.

Howison, S., 1992. "Complex variable methods in hele–shaw moving boundary problems". *European Journal of Applied Mathematics*, Vol. 3, No. 3, pp. 209–224.

Jackson, M., 2021. *Interfacial instability analysis of viscous flows in a Hele-Shaw channel*. Ph.D. thesis, Queensland University of Technology. doi:10.5204/thesis.eprints.212417. URL https://eprints.qut.edu.au/212417/.

Livera, P.O., Anjos, P.H. and Miranda, J.A., 2021. "Magnetically induced interfacial instabilities in a ferrofluid annulus". *Physical Review E*, Vol. 104, No. 6, p. 065103.

Livera, P.O., Anjos, P.H. and Miranda, J.A., 2022. "Ferrofluid annulus in crossed magnetic fields". *Physical Review E*, Vol. 105, No. 4, p. 045106.

McCloud, K.V. and Maher, J.V., 1995. "Experimental perturbations to saffman-taylor flow". *Physics Reports*, Vol. 260, No. 3, pp. 139–185.

Miranda, J.A. and Widom, M., 1998. "Weakly nonlinear investigation of the saffman–taylor problem in a rectangular hele–shaw cell". *International Journal of Modern Physics B*, Vol. 12, No. 09, pp. 931–949.

Morrow, L.C., De Cock, N. and McCue, S.W., 2023. "Viscous fingering patterns for hele-shaw flow in a doubly connected geometry driven by a pressure differential or rotation". *Phys. Rev. Fluids*, Vol. 8, p. 014001. doi:10.1103/PhysRevFluids.8.014001. URL https://link.aps.org/doi/10.1103/PhysRevFluids.8.014001.

Saffman, P.G. and Taylor, G.I., 1958. "The penetration of a fluid into a porous medium or hele-shaw cell containing a more viscous liquid". *Proceedings of the Royal Society of London. Series A. Mathematical and Physical Sciences*, Vol. 245, No. 1242, pp. 312–329.

Ward, T. and White, A.R., 2011. "Gas-driven displacement of a liquid in a partially filled radial hele-shaw cell". *Phys. Rev. E*, Vol. 83, p. 046316. doi:10.1103/PhysRevE.83.046316. URL https://link.aps.org/doi/10.1103/PhysRevE.83.046316.

Zhao, M., Anjos, P.H., Lowengrub, J. and Li, S., 2020. "Pattern formation of the three-layer saffman-taylor problem in a radial hele-shaw cell". *Physical Review Fluids*, Vol. 5, No. 12, p. 124005.

7. RESPONSIBILITY NOTICE

The authors are solely responsible for the printed material included in this paper.